

A Novel Ruthenium Precursor for MOCVD without Seed Ruthenium Layer

Tosoh, Tokyo Research Center
Tokyo Institute of Technology

Tetsuo Shibutami
Noriaki Oshima
Hiroshi Funakubo

1 . Introduction

Ruthenium is considered a most promising electrode material for high - dielectric capacitors such as tantalum pentoxide (Ta_2O_5) and barium strontium titanate [(Ba,Sr)TiO₃] in Gbit-scale dynamic random access memories (DRAMs), because it has low resistivity, excellent chemical stability and good dry etching property. Since Grean *et al.*¹ have reported on the preparation of Ru and RuO₂ films by metalorganic chemical vapor deposition (MOCVD) using triruthenium dodecacarbonyl [Ru₃(CO)₁₂], bis(cyclopentadienyl)ruthenium [Ru(Cp)₂ Cp :cyclopentadienyl], and tri(acetylacetonate)ruthenium [Ru(C₅H₇O₂)₃] precursor, there have been several attempts to deposit Ru film by MOCVD using precursors such as tri(dipivaloylmethanate)ruthenium [Ru(DPM)₃ DPM : dipivaloylmethanate]^{2,3}, tri (octanedionate)ruthenium [Ru(OD)₃ OD : octanedionate]^{4,5} and bis(ethylcyclopentadienyl) ruthenium [Ru(EtCp)₂ EtCp : ethylcyclopentadienyl]^{6,7}. Among those precursors, Ru(EtCp)₂ has attracted attention because it has high vapor pressure and is in a liquid state with low viscosity (approximately 5cP) at room temperature. However, there are several reports for the disadvantage of Ru films deposited using Ru(EtCp)₂ precursor in that it has long incubation time at the initial stage of the growth.^{8,9} In order to avoid the long incubation time, there have been some attempts to deposit MOCVD-Ru film on a seed layer of sputter-deposited Ru⁸.

In the present study, the liquid precursor of (2,4-dimethylpentadienyl)(ethylcyclopentadienyl)ruthenium [Ru(DMPD)(EtCp) DMPD:2,4-dimethylpentadienyl] with liquid state having low viscosity (approximately 6cP) at room temperature, which was a new product we launched as a novel precursor, was prepared and used

for Ru films deposition by MOCVD. In MOCVD process, the deposition characteristics and properties of the Ru films deposited from Ru(DMPD)(EtCp) were compared with those from conventional Ru(EtCp)₂.

2 . Experimental

The molecular structure of Ru(DMPD)(EtCp) and Ru(EtCp)₂ are shown in Fig.1(a) and 1(b), respectively. Ru thin films were deposited on oxidized Si substrates without seed Ru layer by MOCVD at the deposition temperature range from 260 to 500 using Ru(DMPD)(EtCp) and Ru(EtCp)₂ individually. The vapor of the precursor was generated by bubbling method kept at 60 where vapor pressure of Ru(DMPD)(EtCp) and Ru(EtCp)₂ were the same and showed approximately 5.3Pa. This vapor was transferred to the cold wall type CVD reactor chamber

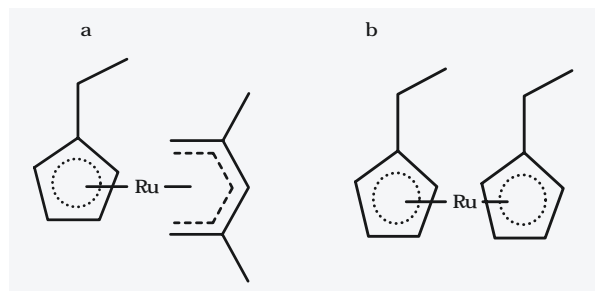


Fig. 1 Molecular structures of (a) Ru(DMPD)(EtCp) and (b) Ru(EtCp)₂.

Table 1 Experimental conditions for Ru film deposition by MOCVD

Precursor	Ru(DMPD)(EtCp)	Ru(EtCp) ₂
Temperature	60	
Carrier gas flow rate	100cm ³ /min	
Pressure	1.33kPa	
Total flow rate	600cm ³ /min	
Dilute gas flow rate	500cm ³ /min	
Deposition temperature	260 ~ 500	

by nitrogen carrier gas. Si wafer covered with 100nm-thick SiO_2 was used as a substrate. The deposition conditions of Ru thin films are summarized in Table 1.

The decomposition temperature of precursors were measured by differential scanning calorimetry (DSC). The crystal structure was identified by X-ray diffraction (XRD). The deposition amount was measured by the X-ray fluorescence (XRF). The resistivity of the Ru films were measured using standard four-probes method. The concentration of carbon impurity in the Ru films were analyzed by secondary ion massspectroscopy (SIMS). The surface morphology was investigated by scanning electron microscopy (SEM).

3 . Results and Discussion

Fig. 2 shows the DSC curves as a function of temperature. The exothermic peak of Ru(DMPD)(EtCp) was started about 80 lower than that from Ru(EtCp)₂. This result indicates that the decomposition temperature of Ru(DMPD)(EtCp) was lower than that of Ru(EtCp)₂.

The Arrhenius plot of the deposition rate are shown

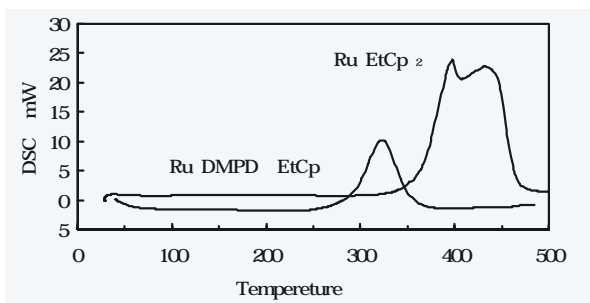


Fig. 2 The DSC curves of Ru(DMPD)(EtCp) and Ru(EtCp)₂ under N₂ atmosphere at a heating rate 10 °C/min.

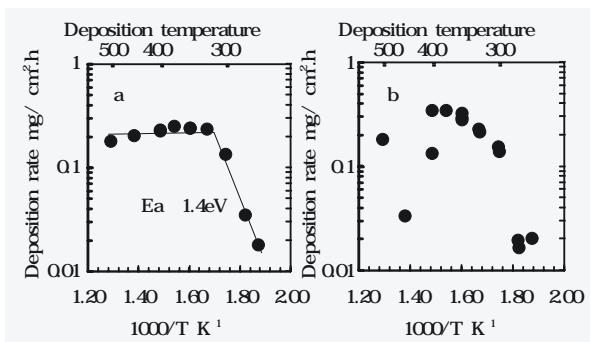


Fig. 3 Arrhenius plot of the deposition rate of Ru films using (a) Ru(DMPD)(EtCp) and (b) Ru(EtCp)₂. Deposition time was 60 min.

in Fig. 3(a) and 3(b) at a deposition temperature of 260 - 500 °C from Ru(DMPD)(EtCp) and Ru(EtCp)₂, respectively. In this case, the film was deposited for 60min. As shown in Fig. 3(a), the deposition rate of Ru films deposited from Ru(DMPD)(EtCp) was constant regardless deposition temperature above 325 °C. This result indicates that deposition in this temperature region dominated by mass-transport-limited process. On the other hand, the deposition rate was decrease with deposition temperature decrease below 300 °C. This phenomenon indicates that the deposition rate is controlled by a reaction-limited process with activation energy (Ea) of approximately 1.4eV. As shown in Fig. 3(b), the deposition rate of the film deposited from Ru(EtCp)₂ was much more unstable than that of Ru(DMPD)(EtCp). Therefore, Ea for Ru(EtCp)₂ could not be estimated.

Fig.4 shows cross-sectional and surface SEM image of the Ru films deposited at 350 °C for 60min. As shown in Fig. 4(a) and 4(c), the grain size and the column width of Ru films deposited from Ru(DMPD)(EtCp) were much smaller than that from Ru(EtCp)₂. The average grain size of Ru films deposited from Ru(DMPD)(EtCp) and Ru(EtCp)₂ were approximately 50nm and 150 nm, respectively.

Fig. 5(a) and 5(b) show X-ray diffraction (XRD) patterns of the same films as shown in Fig. 3 deposited at various deposition temperatures from Ru(DMPD)(EtCp) and Ru(EtCp)₂, respectively. All diffraction peaks could be assigned to be pure Ru phase for both films deposited from Ru(DMPD)(EtCp) and Ru(EtCp)₂.

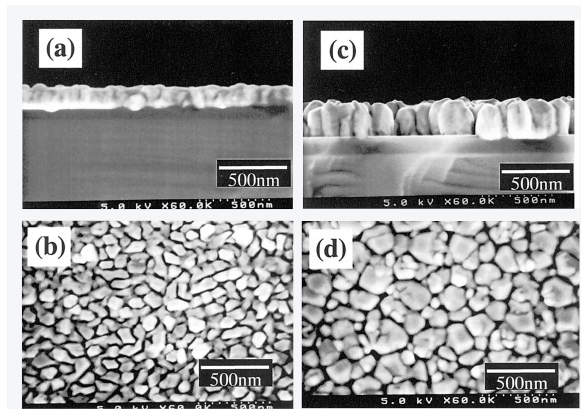


Fig. 4 Cross-sectional and surface SEM images of the Ru films deposited at 350 °C for 60min from (a)(b) Ru(DMPD)(EtCp) and (c)(d) Ru(EtCp)₂.

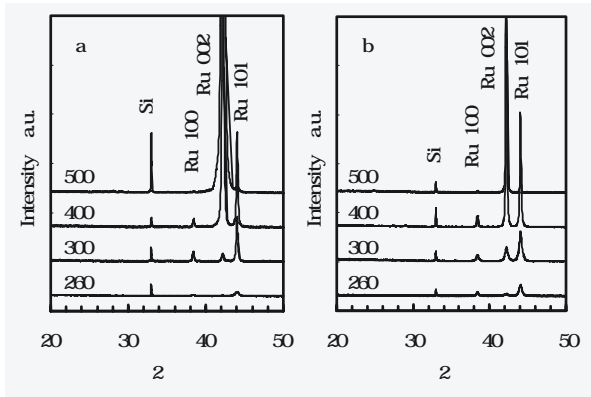


Fig. 5 XRD patterns of Ru thin films deposited at various temperatures from (a) Ru(DMPD)(EtCp) and (b) Ru(EtCp)₂ for 60 min

Fig. 6 shows the variation of the resistivity of the same films as shown in Fig. 3. The resistivity of Ru films deposited from Ru(DMPD)(EtCp) and Ru(EtCp)₂ was high when the deposition temperature was 260 . However, it decreased with the increase of deposition temperature and was under 20 μ cm above 350 .

The amount of carbon ions in the Ru films was analyzed by SIMS. Fig. 7 shows the dependence of average concentration of carbon on deposition temperature. Carbon concentration decreased as deposition temperature increased for the films deposited from both precursors. The carbon concentration was 3 × 10²⁰ atomic/cc for both films above 400 .

Fig. 8 shows SEM images of the first stage of the films deposition at 350 from Ru(DMPD)(EtCp) and Ru(EtCp)₂. As shown in Fig. 8(d), the deposition was hardly observed for 5min deposition when the film was

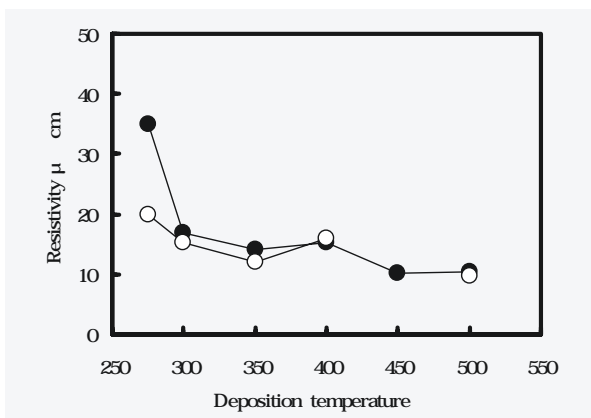


Fig. 6 The resistivity of Ru films deposited from () Ru(DMPD)(EtCp) and () Ru(EtCp)₂.

deposited from Ru(EtCp)₂, while clear deposition was observed from Ru(DMPD)(EtCp). This phenomenon indicates that the deposition process from Ru(EtCp)₂ has longer incubation time than that from Ru(DMPD)(EtCp). This is in good agreement with the previous reports by Matsui *et al.*⁸ and Kadoshima *et al.*⁹. The grain size of Ru films deposited from Ru(DMPD)(EtCp) were much smaller than that from Ru(EtCp)₂. The small grain size of the Ru film deposited from Ru(DMPD)(EtCp) is considered to be due to high nuclear density. This phenomenon indicates that the density of the film deposited from Ru(DMPD)(EtCp) is higher than that from Ru(EtCp)₂.

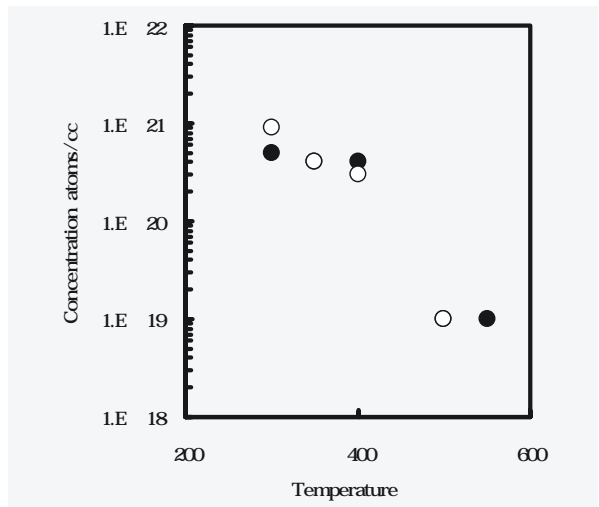


Fig. 7 Average concentration of carbon (determined by SIMS) in Ru films deposited from () Ru(DMPD)(EtCp) and () Ru(EtCp)₂.

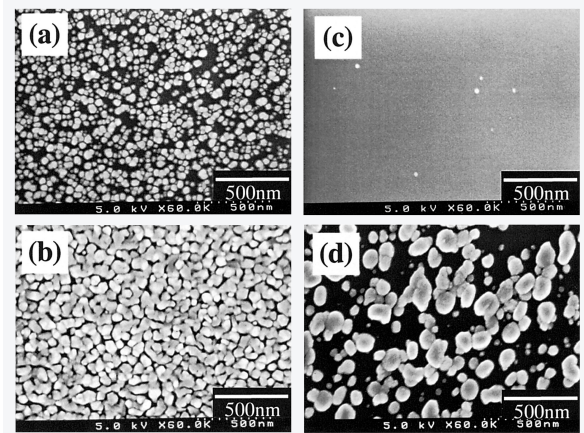


Fig. 8 SEM images of the surface of Ru films deposited at 350 from (a, b) Ru(DMPD)(EtCp) and (c, d) Ru(EtCp)₂ for (a, c) 5min, (b, d) 20min.

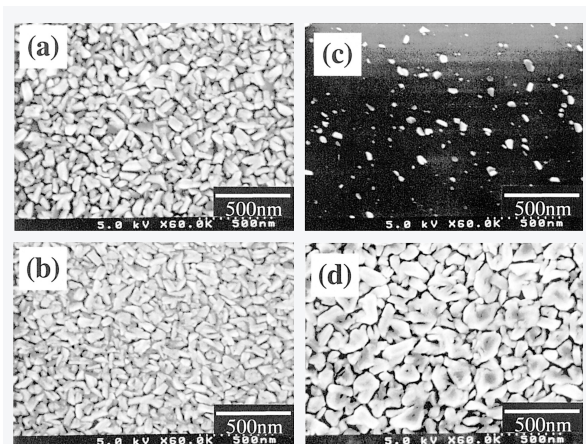


Fig. 9 SEM images of the surface of Ru films deposited at 275 from (a) (b) Ru(DMPD)(EtCp) and (c) (d) Ru(EtCp)₂ for (a) (c) 25min, (b) (d) 35min.

Fig. 9 shows SEM images of the first stage of the films deposition at 275 from Ru(DMPD)(EtCp) and Ru(EtCp)₂. As shown in Fig. 8(c) and Fig. 9(c), the incubation time of Ru films deposited at 275 from Ru(EtCp)₂ was much longer than that deposited at 350. While the clear deposition was observed at 275 from Ru(DMPD)(EtCp).

Fig. 10 shows relationship between the deposition amount of the films and the deposition time for the films deposited at 350 and 275. For both temperatures, the film growth from Ru(EtCp)₂ showed a distinct incubation time compared with that from Ru(DMPD)(EtCp). Furthermore, the incubation time of the films deposited at 275 was longer than that deposited at 350. This results obviously showed that the incubation time from Ru(DMPD)(EtCp) was much shorter than that from Ru(EtCp)₂. The difference of deposition process for Ru(DMPD)(EtCp) and Ru(EtCp)₂ may be presume that the decomposition temperature of Ru(DMPD)(EtCp) was lower than that of Ru(EtCp)₂, which was suggested by DSC data shown in Fig. 2.

4. Conclusions

Ru thin films were deposited by MOCVD using novel liquid precursor of Ru(DMPD)(EtCp) on SiO₂/Si substrate without seed Ru layer at deposition temperature of 260 - 500 together using conventional Ru(EtCp)₂. The films consisted of Ru single phase for the entire deposition temperature range regardless of the starting precursors. The initial stage of Ru films

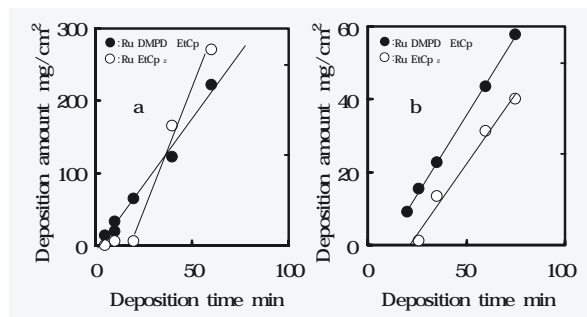


Fig.10 Deposition time dependency of the deposition amount of Ru films deposited at (a) 350 and (b) 275

deposited from Ru(DMPD)(EtCp) precursor was denser than that from Ru(EtCp)₂ precursor. Moreover, the deposition process from Ru(DMPD)(EtCp) had much shorter incubation time than that from Ru(EtCp)₂ when the films were deposited at 275 and 350. This shows that Ru(DMPD)(EtCp) is the novel precursor for MOCVD-Ru film that have dense structure and shorter incubation time. The difference of deposition process for Ru(DMPD)(EtCp) and Ru(EtCp)₂ is considered to be due to difference of decomposition property of those precursor.

References

1. M. L. Green, M. E. Gross, L. E. Papa, K. J. Schnoes, and D. Brasen, *J. Electrochem. Soc.*, 132, 2677(1985).
2. J. M. Lee, J. C. Chin, C. S. Hwang, H. J. Kim, and C. G. Suk, *J. Vac. Sci. Technol. A*, 16, 2768(1998).
3. J. Vetrone, C. M. Foster, G. R. Bai, A. Wang, J. Patel, and X. Wu, *J. Mater. Res.*, 8, 2281(1998).
4. J. H. Lee, J. Y. Kim, S. W. Rhee, D. Y. Yang, D. H. Kim, C. H. Yang, Y. K. Han, and C. J. Hwang, *J. Vac. Sci. Technol. A*, 18, 2400(2000).
5. J. H. Lee, J. Y. Kim, and S. H. Rhee, *J. Electrochem. Solid-State Lett.*, 2, 622(1999).
6. T. Aoyama, and K. Eguchi, *Jpn. J. Appl. Phys.*, 38, L1134(1999).
7. S. Y. Kang, K. H. Choi, S. K. Lee, C. S. Hwang, and H. K. Kim, *J. Electrochem. Soc.*, 147, 1161(2000).
8. Y. Matsui, M. Hiratani, T. Nabatame, Y. Shimamoto, and S. Kimura, *Electrochem. Solid-State Lett.*, 4, C9(2001).
9. M. Kadoshima, T. Nabatame, M. Hiratani, and Y. Nakamura, *Jpn. J. Appl. Phys.*, 41, L347(2002).